Journal of Organometallic Chemistry 695 (2010) 74–81

Contents lists available at ScienceDirect

Journal of Organometallic Chemistry

journal homepage: www.elsevier.com/locate/jorganchem

# Imine-functionalized, fluorescent organomercury and -tellurium compounds

Vadapalli Chandrasekhar *, Arun Kumar, Mrituanjay D. Pandey

*Department of Chemistry, Indian Institute of Technology Kanpur, Kanpur 208 016, India*

ARTICLE INFO

*Article history:*
Received 3 August 2009
Received in revised form 9 September 2009
Accepted 22 September 2009
Available online 29 September 2009

*Keywords:*
Organomercury
Organotellurium
Fluorescence
Pyrene
Anthracene
Phenanthrene

ABSTRACT

Unsymmetrical diorganotellurium(IV) dihalides, Ar′(Ar)$TeCl_2$ [Ar′ = 2-(R-CH=N-$C_6H_3$Me; R = 1-pyrenyl, 9-anthracenyl and 9-phenanthrenyl; Ar = 4-MeO-$C_6H_4$, 1-$C_{10}H_7$, 2,4,6-$Me_3$-$C_6H_2$, $C_6H_5$, 4-Me-$C_6H_4$] were synthesized from transmetallation reactions of Ar′HgCl and $ArTeCl_3$. Orthomercuration of the Schiff's bases (Ar′H) afforded Ar′HgCl. All of these compounds have been characterized with the help of IR, multinuclear ($^1H$, $^{13}C$) solution NMR and ESI-HRMS spectrometry. X-ray crystal structures of pyrenyl Ar′HgCl; pyrenyl Ar′(Ar)$TeCl_2$ (Ar = 4-MeO-$C_6H_4$); anthranyl Ar′(Ar)$TeCl_2$ (Ar = 4-MeO-$C_6H_4$ and 1-$C_{10}H_7$) and; phenathranyl Ar′(Ar)$TeCl_2$ (Ar = 1-$C_{10}H_7$) have been determined. Intramolecular Hg/Te···N interactions are present in these structures. Fluorescence studies of these compounds have also been carried out.



## 1. Introduction

There has been some interest recently in the preparation of main-group organometallic compounds containing a functional periphery [1]. Cyclophosphazenes and organostannoxanes have, for example, been used as scaffolds to support a variety of interesting groups that are electrochemically or photochemically active [2,3]. Organostannoxanes containing photoactive substituents have been shown to possess interesting photochemical behavior in solution as well as in the solid state [3–7]. Such a methodology has not yet been applied to the realm of organotellurium chemistry. Recent reports on the preparation of interesting organotellurium compounds such as tellurinic acids indicate a new resurgence in organotellurium chemistry [8a]. In view of this we were interested in exploring methodologies that would allow the preparation of organotellurium compounds possessing photoactive substituents. Accordingly in this paper we adopted the orthomercuration strategy of Schiff bases followed by transmetallation reactions [8b–d] to afford various types of organotellurium dihalides, [2-{*N*-(1-pyrenylmethylene)-4-methyl} -benzenamine](aryl) tellurium(IV) dichloride, [aryl = 4-MeO-$C_6H_4$, **1a**; 1-$C_{10}H_7$, **1b**; 2,4,6-$Me_3$-$C_6H_2$, **1c**; $C_6H_5$, **1d**; 4-Me-$C_6H_4$, **1e**]; [2-{*N*-(9-anthracenylmethylene)-4-methyl}-benzenamine](aryl)tellurium(IV) dichloride, [aryl = 4-MeO-$C_6H_4$, **2a**; 1-$C_{10}H_7$, **2b**; 2,4,6-$Me_3$-$C_6H_2$, **2c**]; [2-{*N*-(9-phenanthrenylmethylene)-4-methyl}-benzenamine](aryl) tellurium(IV) dichloride, [aryl = 4-MeO-$C_6H_4$, **3a**; 1-$C_{10}H_7$, **3b**; 2,4,6-$Me_3$-$C_6H_2$, **3c**]. Representative examples of organomercury and tellurium compounds have been structurally characterized in the solid state by single-crystal X-ray diffraction. The solution state photophysical properties of these compounds are also reported.

## 2. Results and discussion

### 2.1. Synthesis

Schiff bases **SB-1**, **SB-2** and **SB-3** have been prepared using a regular synthetic procedure or a protocol involving the microwave reactor (see Section 4) (Scheme 1). Orthomercuration of the Schiff bases was achieved by their reaction with $Hg(CH_3COO)_2$ followed by treatment with LiCl. This procedure afforded the organomercury compounds **1**–**3** (Scheme 1) each of which contained an Hg–Cl bond. While **1** was characterized by single-crystal X-ray diffraction method (*vide infra*) the insolubility of **2** and **3** precluded attempts to obtain their crystals. Transmetallation of **1**–**3** with $ArTeCl_3$ (Ar = 4-MeO-$C_6H_4$, 1-$C_{10}H_7$, 2,4,6-$Me_3$-$C_6H_2$, $C_6H_5$, 4-Me-$C_6H_4$) afforded the organotellurium dichlorides **1a**–**1e**, **2a**–**2c** and **3a**–**3c** (Scheme 1). These compounds are air stable and are sparingly soluble in common organic solvents such as $CH_2Cl_2$, $CHCl_3$, $(CH_3)_2CO$ as well hydrocarbons. However, they are soluble in acetonitrile, dimethylformamide and dimethylsulfoxide. Molecular structures of **1**, **1a**, **2a**, **2b** and **3b** could be established by single-crystal X-ray diffraction. The IR and NMR data of these compounds are summarized in Section 4 and are unexceptional.

* Corresponding author. Tel.: +91 512 259 7259; fax: +91 521 259 0007x7436.
*E-mail address:* vc@iitk.ac.in (V. Chandrasekhar).

0022-328X/$ - see front matter © 2009 Elsevier B.V. All rights reserved.
doi:10.1016/j.jorganchem.2009.09.030

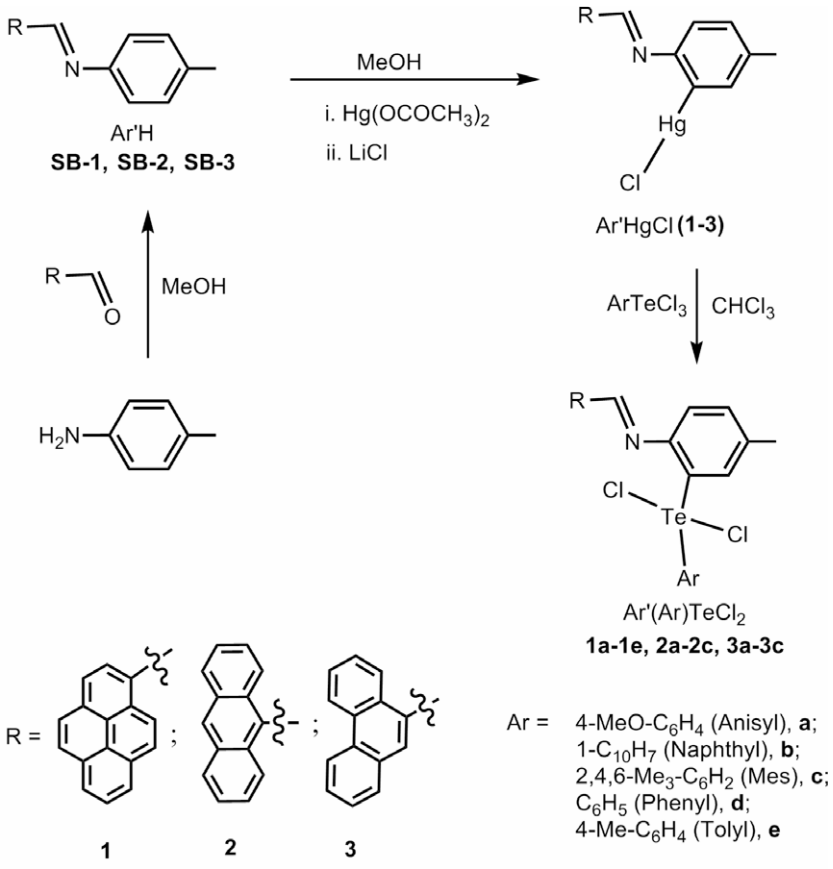


**Scheme 1.**

### 2.2. Molecular and crystal structures of *1*, *1a*, *2a*, *2b* and *3b*

The crystallographic data and refinement parameters of **1**, **1a**, **2a**, **2b** and **3b** are summarized in Table 1. Selected bond length and angle data for these compounds are presented in Table 2. ORTEP diagrams of these compounds are shown in Figs. 1–5. A brief description of the structural aspects of these compounds is presented below.

The asymmetric unit of **1** contains two symmetry-related crystallographically independent molecules. The mercury center has a linear geometry [9a] with weak secondary intramolecular Hg···N interaction (3.014(11) Å) in a four-membered ring (Fig. 1). While this distance is only slightly smaller than the sum of the van der Waals radii of mercury and nitrogen (3.05 Å) [9b] and is certainly smaller than many analogous intramolecular Hg···N contacts, [10,11] we believe that a weak interaction does exist between Hg and N. The corresponding motifs N1–C2 and Te–Cl bend towards each other which is reflected in the >120° angles observed for N–C–C (~117.6°) and C–C–Hg (~116.0°). Interestingly while in one of the molecules all the non-hydrogen atoms lie in the same plane, in the second molecule a dihedral angle of ~42° is found between two planar segments that are linked by the CH=N unit. C–H···Cl, Hg···π and Hg···Cl interactions organize the molecules into a three-dimensional supramolecular structure (Supplementary material).

The molecular structures of the diorganotellurium dichlorides are grossly similar (Figs. 2–5). In all the cases the geometry around tellurium can be considered as distorted trigonal bipyramidal if one takes into account the stereochemically active lone pair. The electronegative chloride ligands occupy the axial positions while the carbon atoms belonging to the aromatic substituents occupy the equatorial positions. It can be seen that the equatorial bond angles are distorted more than the axial ones (axial Cl–Te–Cl bond angles: **1a**: 174.77(6)°; **2a**: 175.27(5)°; **2b**: 173.04(6)°; **3b**: 170.71(5)°; equatorial C–Te–C bond angles: **1a**: 98.6(2)°; **2a**: 95.2(2)°; **2b**: 101.6(2)°; **3b**: 101.54(2)°). The distortion of the equatorial angles is mainly due to the presence of the lone pair of electrons in the equatorial plane. In all the cases a strong Te···N interaction is seen (**1a**: 2.914(5); **2a**: 2.983(6); **2b**: 2.876(6) and **3b**: 2.967(5) Å). These distances are much shorter than the sum of the van der Waals radii of Te and N atoms (3.7 Å) [12]. The intramolecular Te···N distances observed in the present instance are comparable with literature precedents [13,14].

The supramolecular structures of the tellurium compounds reveal that non covalent intermolecular interactions involving Te atom are absent. C–H···Cl, C–H···π and π···π interactions play a leading role in the supramolecular architectures (see Supplementary material). For illustration the supramolecular organization of **2a** is described; the rest are presented in Supplementary material. In **2a** a centrosymmetric dimer is first formed as a result of reciprocatory intermolecular C–H···Cl (H···Cl = 2.923(1) Å) interactions (Fig. 6a). Such dimers are organized into a one-dimensional supramolecular structure by bifurcated C–H···Cl···H–C interaction (Fig. 6b). The chlorine atom involved in this is extended into a trifurcated C–H···Cl interaction (Fig. 6c). Additional π···π stacking between the aromatic rings of the anisyl substituents results in a 3D-architecture (Fig. 6d). This hierarchal organization is depicted in Fig. 6.

### 2.3. Absorption and emission spectroscopy

Absorption spectra of all the compounds were recorded in their acetonitrile solutions in $10^{-5}$ M concentrations. This data are summarized in Table 3. The Schiff bases **SB-1**, **SB-2** and **SB-3** show

**Table 1**
X-ray crystallographic data for compounds **1**, **1a**, **2a**, **2b** and **3b**.

| | **1** | **1a** | **2a** | **2b** | **3b** |
|---|---|---|---|---|---|
| Empirical formula | $C_{24}H_{16}ClHgN$ | $C_{31}H_{23}Cl_2NOTe$ | $C_{29}H_{23}Cl_2NOTe$ | $C_{66}H_{46}Cl_4N_2O_9\ Te_2$ | $C_{32}H_{23}Cl_2NTe$ |
| Formula weight | 554.42 | 624 | 599.98 | 1408.05 | 620.01 |
| Temperature (K) | 273(2) | 100(2) | 100(2) | 100(2) | 100(2) |
| Wavelength (Å) | 0.71073 | 0.71073 | 0.71069 | 0.71073 | 0.71073 |
| Crystal system | Triclinic | Triclinic | Triclinic | Triclinic | Monoclinic |
| Space group | $P\bar{1}$ | $P\bar{1}$ | $P\bar{1}$ | $P\bar{1}$ | $C2/c$ |
| $a$ (Å) | 8.449(3) | 8.4804(9) | 8.990(5) | 7.618(3) | 33.392(10) |
| $b$ (Å) | 14.601(5) | 8.9301(9) | 10.213(5) | 13.128(4) | 7.634(2) |
| $c$ (Å) | 15.688(5) | 17.1533(18) | 13.234(5) | 15.219(5) | 20.101(6) |
| $\alpha$ (°) | 80.134(6) | 77.546(2) | 91.644(5) | 105.680(5) | 90 |
| $\beta$ (°) | 82.448(6) | 84.220(2) | 93.221(5) | 104.380(6) | 100.667(7) |
| $\gamma$ (°) | 85.401(6) | 79.966(2) | 95.517(5) | 95.868(5) | 90 |
| $V$ (Å$^3$) | 1886.8(11) | 1246.4(2) | 1206.8(10) | 1395.9(8) | 5035(3) |
| $Z$ | 4 | 2 | 2 | 1 | 8 |
| $D_{calcd.}$ (g cm$^{-3}$) | 1.952 | 1.663 | 1.651 | 1.675 | 1.636 |
| $\mu$ (mm$^{-1}$) | 8.307 | 1.434 | 1.478 | 1.300 | 1.417 |
| $F$(0 0 0) | 1056 | 620 | 596 | 700 | 2464 |
| Crystal size (mm) | 0.088 × 0.072 × 0.053 | 0.08 × 0.04 × 0.03 | 0.09 × 0.06 × 0.04 | 0.09 × 0.06 × 0.04 | 0.10 × 0.06 × 0.03 |
| $\theta$ Range (°) | 2.09–28.40 | 2.36–27.00 | 2.28–27.00 | 2.50–26.00 | 2.20–28.38 |
| Limiting indices | $-11 \leqslant h \leqslant 10$, $-12 \leqslant k \leqslant 19$, $-20 \leqslant l \leqslant 20$ | $-10 \leqslant h \leqslant 5$, $-11 \leqslant k \leqslant 9$, $-21 \leqslant l \leqslant 21$ | $-11 \leqslant h \leqslant 10$, $-12 \leqslant k \leqslant 12$, $-16 \leqslant l \leqslant 16$ | $-9 \leqslant h \leqslant 9$, $-16 \leqslant k \leqslant 16$, $-18 \leqslant l \leqslant 16$ | $-42 \leqslant h \leqslant 44$, $-9 \leqslant k \leqslant 10$, $-18 \leqslant l \leqslant 26$ |
| Reflections collected | 12 202 | 7468 | 7157 | 7749 | 15 933 |
| Independent reflections [$R_{(int)}$] | 8936 [0.0487] | 5248 [0.0247] | 5065 [0.0245] | 5331 [0.0274] | 6202 [0.0641] |
| Refinement method | Full-matrix least-squares on $F^2$ | Full-matrix least-squares on $F^2$ | Full-matrix least-squares on $F^2$ | Full-matrix least-squares on $F^2$ | Full-matrix least-squares on $F^2$ |
| Data/restraints/parameters | 8936/0/490 | 5248/0/327 | 5065/0/307 | 5331/0/347 | 6202/0/325 |
| Goodness-of-fit (GOF) on $F^2$ | 1.032 | 1.127 | 1.151 | 1.117 | 1.075 |
| Final $R$ indices [$I > 2\sigma(I)$] | $R_1$ = 0.0699, $wR_2$ = 0.1858 | $R_1$ = 0.0506, $wR_2$ = 0.1310 | $R_1$ = 0.0498, $wR_2$ = 0.1397 | $R_1$ = 0.0654, $wR_2$ = 0.1732 | $R_1$ = 0.0495, $wR_2$ = 0.1083 |
| R indices (all data) | $R_1$ = 0.1375, $wR_2$ = 0.2585 | $R_1$ = 0.0675, $wR_2$ = 0.1805 | $R_1$ = 0.0644, $wR_2$ = 0.2062 | $R_1$ = 0.0813, $wR_2$ = 0.1960 | $R_1$ = 0.0863, $wR_2$ = 0.1428 |

**Table 2**
Selected bond lengths (Å) and angles (°) for **1**, **1a**, **2a**, **2b** and **3b**.

| | **1** | | **1a** | **2a** | **2b** | **3b** |
|---|---|---|---|---|---|---|
| Hg1–C2 | 2.030(14) | C17–Te | 2.116(7) | 2.124(7) | 2.109(6) | 2.095(5) |
| Hg2–C26 | 2.065(12) | C23–Te | 2.122(7) | 2.117(6) | 2.122(7) | 2.137(5) |
| Hg1–Cl1 | 2.320(5) | Cl1–Te | 2.4878(18) | 2.5075(19) | 2.4512(19) | 2.4603(15) |
| Hg2–Cl2 | 2.326(4) | Cl2–Te | 2.5160(17) | 2.5033(18) | 2.5864(18) | 2.5428(14) |
| Hg1···N1 | 3.0133(128) | C15–N | 1.267(8) | 1.288(9) | 1.274(9) | 1.306(6) |
| Hg2···N2 | 3.0142(112) | C16–N | 1.400(8) | 1.424(8) | 1.426(8) | 1.409(7) |
| C2–C1–N1 | 118.9(13) | Te···N | 2.91499(47) | 2.9827(56) | 2.8764(63) | 2.9670(49) |
| C1–C2–Hg1 | 115.4(11) | C17–Te–C23 | 98.6(3) | 95.2(2) | 101.6(2) | 101.54(19) |
| C2–Hg1–Cl1 | 176.9(4) | Cl1–Te–Cl2 | 174.77(6) | 175.27(5) | 173.04(6) | 170.71(5) |
| C26–C25–N2 | 116.3(11) | C17–Te–Cl1 | 87.86(19) | 89.57(17) | 89.45(18) | 89.99(13) |
| C25–C26–Hg2 | 116.5(9) | C23–Te–Cl1 | 90.4(2) | 92.07(18) | 89.38(19) | 86.14(14) |
| C26–Hg2–Cl2 | 177.0(3) | C17–Te–Cl2 | 86.91(18) | 86.99(17) | 84.36(18) | 85.53(13) |
| C26–Hg2···N2 | 52.910(401) | C23–Te–Cl2 | 90.5(2) | 91.48(18) | 88.76(18) | 86.79(14) |
| C25–N2···Hg2 | 74.264(650) | C15–N–C16 | 122.6(6) | 118.2(5) | 121.2(6) | 118.0(4) |
| C2–Hg1···N1 | 53.111(475) | C17–C16–N | 116.9(6) | 116.0(5) | 115.0(6) | 114.8(4) |
| C1–N1···Hg1 | 72.534(773) | C21–C16–N | 122.7(6) | 126.9(6) | 126.7(6) | 128.2(4) |
| | | C16–C17–Te | 112.6(5) | 114.4(4) | 111.9(4) | 115.3(4) |
| | | C18–C17–Te | 124.6(5) | 123.2(5) | 125.3(5) | 123.3(3) |
| | | C24–C23–Te | 120.8(5) | 121.2(5) | 120.5(5) | 118.8(4) |
| | | C28–C23–Te | 118.5(5) | 120.3(5) | | |
| | | C31–C23–Te1 | | | 117.5(5) | 118.1(4) |
| | | C16–N···Te | 77.047(345) | 76.666(328) | 78.238(364) | 77.174(271) |
| | | C17–Te···N | 53.401(217) | 52.931(199) | 54.676(190) | 52.694(154) |

absorption in the following manner: **SB-1**: 278 ($\varepsilon = 4.3 \times 10^{-4}$), 289 ($\varepsilon = 4.5 \times 10^{-4}$), 375 ($\varepsilon = 3.7 \times 10^{-4}$), 398 ($\varepsilon = 2.8 \times 10^{-4}$); **SB-2**: 226 ($\varepsilon = 2.7 \times 10^{-4}$), 394 ($\varepsilon = 1.0 \times 10^{-4}$); **SB-3**: 330 ($\varepsilon = 9.5 \times 10^{-4}$). These spectra are shown in Fig. 7 and are typical of polyaromatic compounds. The absorptions arise mainly due to $\pi$–$\pi^*$ transitions of the signaling subunits [15].

Mercuration of **SB-1** leads to a slight red-shift for one of the bands at 398 nm, while telluration reverts back this peak position (Table 3). In contrast the trends seen in the anthracene derivatives are exactly the opposite (Table 3). However, the phenanthrene derivatives follow the same trend as observed for the pyrene compounds.

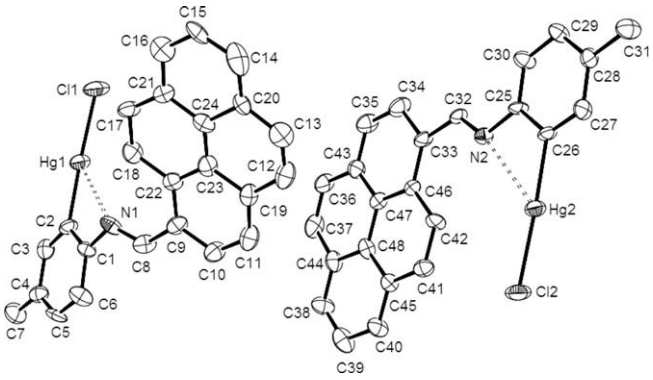


**Fig. 1.** ORTEP diagram of **1** with 50% thermal ellipsoids. Hydrogen atoms have been omitted for clarity.

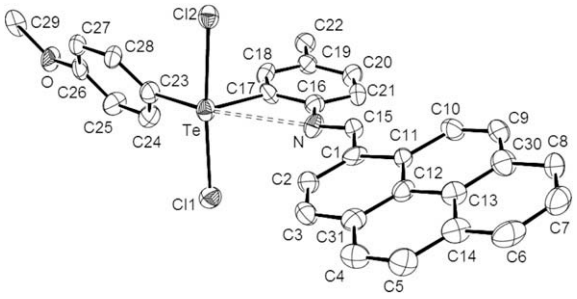


**Fig. 2.** ORTEP diagram of **1a** with 50% thermal ellipsoids. Hydrogen atoms have been omitted for clarity.

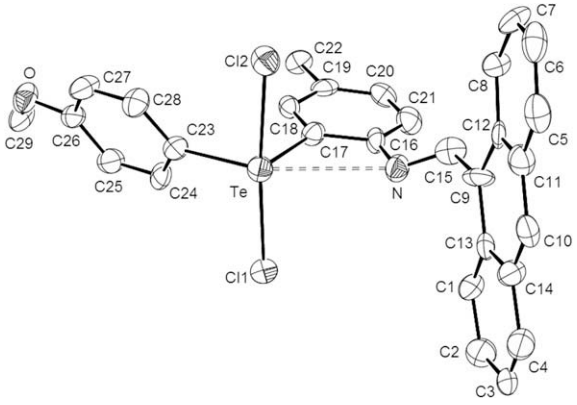


**Fig. 3.** ORTEP diagram of **2a** with 50% thermal ellipsoids. Hydrogen atoms have been omitted for clarity.

Fluorescence spectra of the pyrene compounds were obtained by using an excitation wavelength of 375 nm while that of the anthracene and phenanthrene derivatives were obtained by exciting at 330 nm. The emission data along with quantum yields are given in Table 3. The quantum yields were calculated using anthracene as the reference. Pyrene-containing compounds show a broad emission in the range $\lambda_{em}$ 415–421 nm. The emission maxima as well as the overall shape of the fluorescence band are not greatly affected by mercuration or telluration showing the dominant effect of the pyrene fluorophore. In contrast in the anthracene derivatives, while the parent Schiff base shows a broad emission at $\lambda_{em}$ = 436 nm, upon metallation two emission bands are shown around 406 and 425 nm. In all the phenanthrene derivatives, including the unmetallated Schiff bases, two separate emission

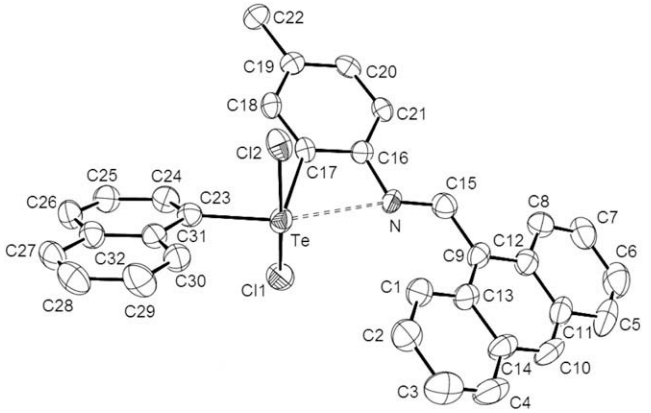


**Fig. 4.** ORTEP diagram of **2b** with 50% thermal ellipsoids. Hydrogen atoms and solvents have been omitted for clarity.

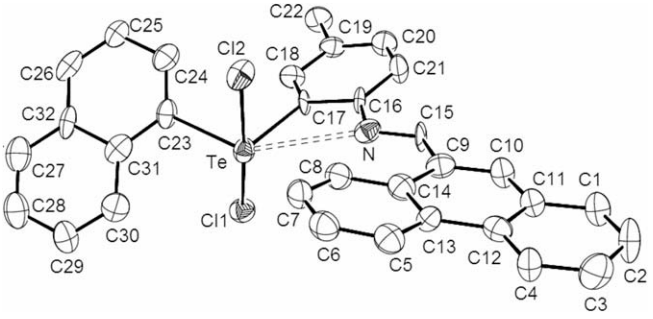


**Fig. 5.** ORTEP diagram of **3b** with 50% thermal ellipsoids. Hydrogen atoms have been omitted for clarity.

peaks are seen around 406 and 425 nm. In general, it has been observed earlier, that metalation of polyaromatic group containing Schiff base ligands results in quenching of the fluorescence particularly with paramagnetic metal ions [16]. This quenching is attributed to the formation of a fluorophore–metal interaction mediated by the π-electrons of the fluorophore [17]. In the current instance also the literature trends are generally followed. Exceptions, however, are found for **1b**, **3b** and **3c** where the emission intensity is increased slightly (Table 3 and Fig. 8). However, these changes are not significantly high and at this moment we are unable to rationalize this result.

## 3. Conclusions

In conclusion we have successfully prepared several fluorophore-containing organomercury chlorides and diaryltellurium dichlorides. The value of these compounds lies in the fact that attaching the heavy metal unit to the fluorophore does not affect, in any significant manner, the fluorescence property of the Schiff base ligands. These compounds as such or their oxo forms are potential ligands for coordination to metal ions. It is anticipated that the fluorophore present in these new family of ligands would be extremely sensitive to interaction with metal ions, which might enable selective sensing of metal ions. These studies are in progress.

## 4. Experimental

### 4.1. Reagents and general procedures

Preparative work was carried out under dry nitrogen using anhydrous solvents. Solvents were purified by standard procedures

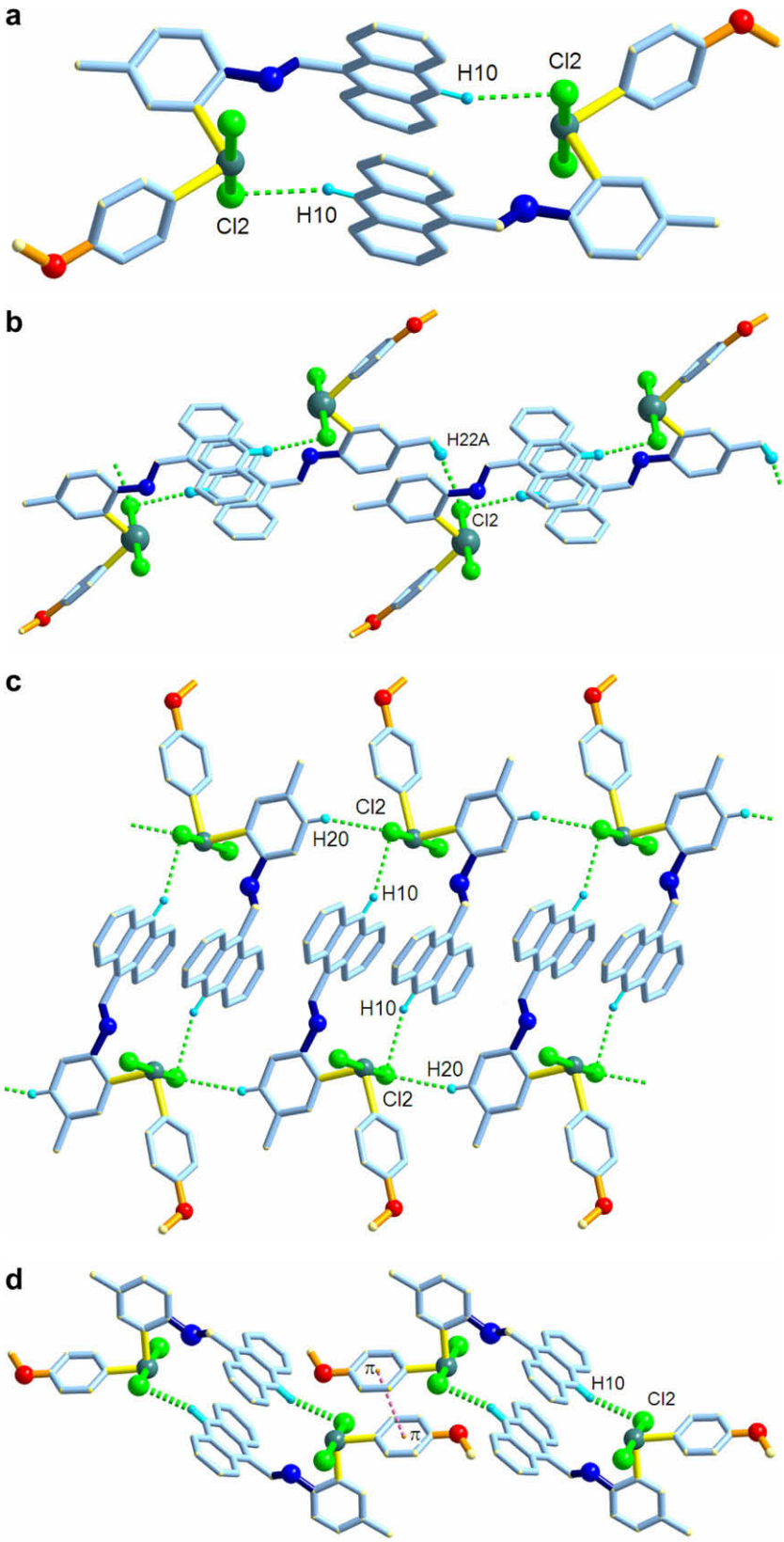


**Fig. 6.** (a) A centrosymmetric dimeric unit realized through C–H···Cl interactions, (b) 1-D chain from dimeric unit by bifurcated C–H···Cl interactions in (c) C–H···Cl interactions present in 3D packing and (d) Slipped π···π stacking between anisyl rings connecting dimeric unit in **2a**.

and stored under $N_2$ over activated molecular sieves [18]. Pyrene-1-carboxaldehyde, anthracene-9-carboxaldehyde, phenanthrene-9-carboxaldehyde, tellurium tetrachloride, tellurium powder, magnesium-metal, bromobenzene, 4-bromotoluene, 1-bromonaphthalene, 2-bromomesitylene and sulfuryl chloride were purchased from Aldrich Chemical Co. (USA) and were used as received. Ani-

**Table 3**
Photophysical data.

| Compounds | $\lambda_{max}$ (nm); ($\varepsilon$) | $\lambda_{em}$ (nm) | $\varphi_F$ |
|---|---|---|---|
| **SB-1** | 278 (42 554), 289 (45 133), 375 (36 944), 398 (27 982) | 421 | 0.0080 |
| **1** | 281 (23 276), 289 (23 888), 380 (17 972), 404 (15 392) | 420 | 0.0078 |
| **1a** | 277 (16 748), 286 (17 360), 375 (9928), 391 (10 234) | 418 | 0.0053 |
| **1b** | 275 (34 204), 300 (17 811), 361 (7043), 373 (6431), 392 (4916) | 415 | 0.0102 |
| **1c** | 275 (19 487), 287 (22 212), 376 (16 602), 394 (18 729), 420 (16 150) | 418 | 0.0065 |
| **1d** | 278 (14 635), 287 (18 729), 375 (12 201), 390 (12 056) | 421 | 0.0042 |
| **SB-2** | 394 (100 000) | 436 | 0.0064 |
| **2** | 336 (20 000) | 404, 423 | 0.0052 |
| **2a** | 411 (10 000) | 406, 426 | 0.0054 |
| **2b** | 405 (6000) | 407, 425 | 0.0060 |
| **2c** | 330 (10 000), 371 (21 000), 404 (27 000) | 406, 426 | 0.0045 |
| **SB-3** | 330 (95 000) | 407, 425 | 0.0053 |
| **3** | 404 (600) | 406, 426 | 0.0045 |
| **3a** | 330 (8500), 520 (4000) | 405, 424 | 0.0022 |
| **3b** | 305(16 000), 522 (5000) | 407, 425 | 0.0051 |
| **3c** | 312 (20 000) | 407, 423 | 0.0060 |

sole was purchased from s.d. Fine. Chem. Ltd., Mumbai, India and distilled under $N_2$ atmosphere before use. $Hg(CH_3COO)_2$, LiCl and *p*-toluidine (RANKEM) were purchased from RFCL Limited, New Delhi, India and were used as such. $ArTeCl_3$ (Ar = $C_6H_5$, 4-Me-$C_6H_4$, 4-$C_{10}H_7$, 2,4,6-$Me_3$-$C_6H_2$) were prepared by the chlorination of their corresponding ditellurides [19–21]. However, 4-MeO-$C_6H_4TeCl_3$ was prepared from a direct reaction of $TeCl_4$ and anisole [22]. Fluorescence and electronic spectra were recorded on a Varian Luminescence Cary eclipsed and Perkin–Elmer-Lambda 20 UV–Vis spectrophotometer, respectively, by using a 10 mm quartz cell at room temperature. Some of the reactions were carried out in Laboratory Microwave Reactor, Discover BenchMate System, make: CEM corp. USA. Melting points were recorded by using a JSGW melting point apparatus in capillary tubes and are uncorrected. IR spectra were recorded as KBr pellets with a Bruker Vector 22 FTIR spectrophotometer operating from 4000–400 $cm^{-1}$. Electrospray ionization – high resolution mass (ESI-HRMS) spectra were recorded with a WATERS-HAB213 spectrometer by using capillary 2.7 kV. NMR ($^1H$, $^{13}C$) spectra were recorded with a JEOL JNM LAMBDA 400 model spectrometer or a JEOL-DELTA2 500 model spectrometer.

### 4.2. Syntheses

#### 4.2.1. Syntheses of Schiff bases, (*SB-1*, *SB-2* and *SB-3*)

A solution of the arene carboxaldehyde, 1 mmol (arene = pyrene-1-: 0.23 g; anthracene-9-: 0.20 g; phenanthrene-9-: 0.20 g) in methanol (~20 ml) and 4-toluidene (0.11 g, 1 mmol) were mixed together. The resulting suspension was stirred in a microwave reactor in a sealed vessel at 120 °C for 10–12 min. Then the resulting solution was stirred at room temperature for ~5 min. A yellow solid separated which was filtered and washed with ice-cold methanol followed by diethyl ether. Recrystallization from chloroform afforded the respective Schiff bases as yellow crystalline solids. An alternative procedure of preparing these compounds involves refluxing the reaction mixture for ~8 h. No significant change in

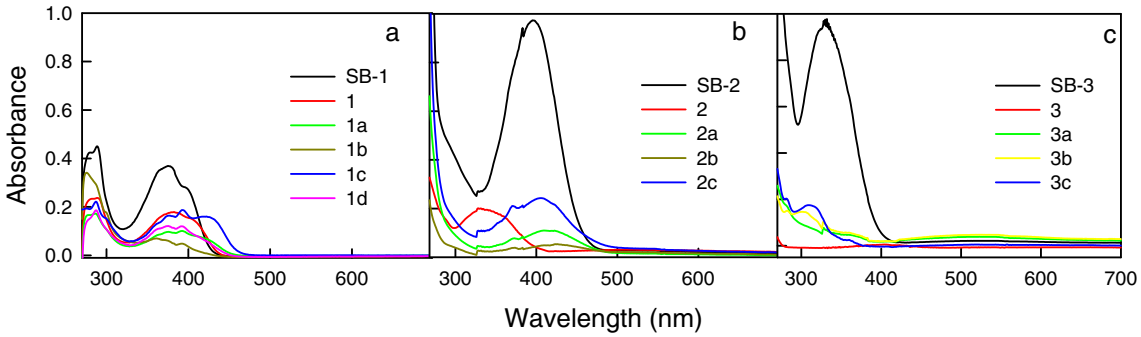


**Fig. 7.** UV–Vis spectra of (a) pyrene (**1a–1e**), (b) anthracene (**2a–2c**) and (c) phenanthrene (**3a–3c**) derivatives in acetonitrile (concentration ~ 10 μM).

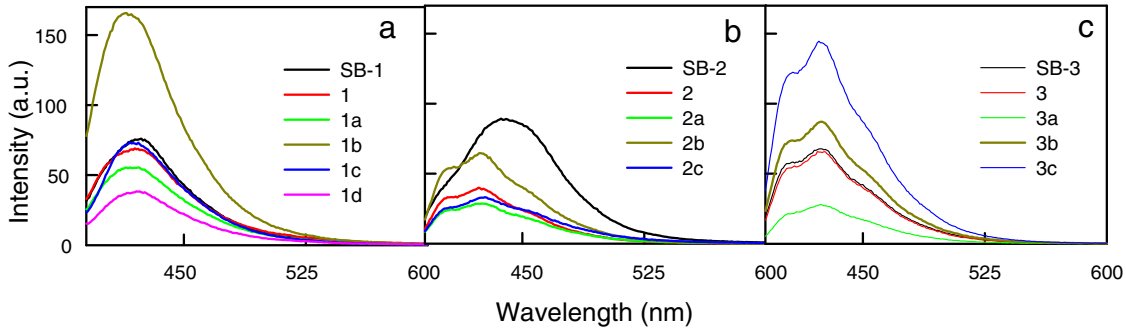


**Fig. 8.** Fluorescence spectra of (a) pyrene (**1a–1e**) (excitation wavelength: 375 nM), (b) anthracene (**2a–2c**) (excitation wavelength: 330 nM) and (c) phenanthrene (**3a–3c**) (excitation wavelength: 330 nM) derivatives in acetonitrile (concentration of 10 μM).

yields was noticed. The following are the data pertaining to these compounds. The yields pertain to the microwave method.

*4.2.1.1. 4-Methyl-N-(pyrene-1-ylmethylene)aniline (SB-1).* Yield: 0.29 g (91%); M.p.: 132 °C. IR (KBr)/cm$^{-1}$: $\nu_{asym}$ (CH=N): 1616.7. $^1$H NMR (400 MHz, $CDCl_3$): $\delta$ 2.36 (s, Me), 7.18–8.97 (m, aryl), 9.44 (s, CH=N) ppm. $^{13}$C NMR (500 MHz, DMSO-$d_6$): 21.5 (Me), 121.0, 122.4, 125.1, 125.9, 126.1, 126.2, 126.6, 127.1, 127.2, 127.5, 128.9, 129.7 (*i*-pyrene), 129.9 (*p*-tolyl), 130.9 (*i*-tolyl), 158.1 (CH=N) ppm. ESI-HRMS: $m/z$ = 320.1437 (found), 320.1439 (calculated) for $[M+H]^+$. Anal. Calc. for $C_{24}H_{17}N$ (319.40): C, 90.25; H, 5.36; N, 4.39. Found: C, 90.12; H, 5.53; N, 4.51%.

*4.2.1.2. 4-Methyl-N-(anthracene-9-ylmethylene)aniline (SB-2).* Yield: 0.27 g (92%); M.p.: 103 °C (105 °C, lit. [23]). IR (KBr)/cm$^{-1}$: $\nu_{asym}$ (CH=N): 1620.7. $^1$H NMR (500 MHz, DMSO-$d_6$): $\delta$ 2.21 (s, Me), 6.82–9.12 (m, aryl), 9.21 (s, CH=N) ppm. $^{13}$C NMR (500 MHz, DMSO-$d_6$): 22.4 (Me), 121.7, 121.9, 123.2, 128.3, 128.7, 129.6, 130.1, 130.4, 130.9, 132.2 (*i*-anthracene), 133.0 (*p*-tolyl), 134.5 (*i*-tolyl), 161.7 (CH=N) ppm. ESI-HRMS: $m/z$ = 296.1444 (found), 296.1439 (calculated) for $[M+H]^+$. Anal. Calc. for $C_{22}H_{17}N$ (295.38): C, 89.46; H, 5.80; N, 4.74. Found: C, 90.01; H, 5.60; N, 4.78%.

*4.2.1.3. 4-Methyl-N-(phenanthrene-9-ylmethylene)aniline (SB-3).* Yield: 0.26 g (88%); M.p.: 142 °C. IR (KBr)/cm$^{-1}$: $\nu_{asym}$ (CH=N): 1625.0. $^1$H NMR (500 MHz, DMSO-$d_6$): $\delta$ 2.32 (s, Me), 6.89–8.91 (m, aryl), 9.31 (s, CH=N) ppm. $^{13}$C NMR (500 MHz, DMSO-$d_6$): 21.9 (Me), 122.1, 122.8, 124.7, 125.2, 125.7, 126.5, 127.3, 127.8, 128.1, 128.3, 129.5, 130.0 (*i*-phenanthrene), 131.2 (*p*-tolyl), 131.7 (*i*-tolyl), 160.8 (CH=N) ppm. ESI-HRMS: $m/z$ = 328.1712 (found), 328.1701 (calculated) for $[M+MeOH+H]^+$. Anal. Calc. for $C_{22}H_{17}N$ (295.38): C, 89.46; H, 5.80; N, 4.74. Found: C, 89.83; H, 5.67; N, 4.58%.

*4.2.2. Syntheses of the organomercury compounds **1**–**3***

0.5 mmol of the Schiff base (**SB-1**: 0.16 g, **SB-2**: 0.15 g, **SB-3**: 0.15 g) and mercury(II) acetate (0.17 g, 0.51 mmol) were stirred (24 h) together in refluxing methanol (~40 ml). The reaction mixture was cooled and LiCl (0.05 g, 1.2 mmol) in hot methanol was added under stirring. The resulting precipitate was filtered, washed with diethyl ether and dried. The solid obtained was extracted by hexane *via* a G-4 soxlet frit to avoid the impurity of salts. Recrystallization from $CHCl_3$–MeOH (1:1) solution gave the organomercury compounds **1**–**3** as yellow needles.

**1**, Yield: 0.19 g (68%); M.p.: 222–225 °C. IR (KBr)/cm$^{-1}$: $\nu_{asym}$ (CH=N): 1609.1. $^1$H NMR (500 MHz, $CDCl_3$): $\delta$ 2.36 (s, Me), 7.12–9.02 (m, aryl), 9.62 (s, CH=N). $^{13}$C NMR (500 MHz, $CDCl_3$): 21.0 (Me), 158.2 (CH=N) ppm. ESI-HRMS: $m/z$ = 556.0759 (found), 556.0756 (calculated) for $[M+H]^+$; 839.2335 (found), 839.2350 (calculated) for $[M(-Cl)+SB]^+$.

**2**, Yield: 0.21 g (82%); M.p.: 178–179 °C. IR (KBr)/cm$^{-1}$: $\nu_{asym}$ (CH=N): 1612.4. $^1$H NMR (500 MHz, $CDCl_3$): $\delta$ 2.32 (s, Me), 6.93–8.87 (m, aryl), 9.52 (s, CH=N). $^{13}$C NMR (500 MHz, $CDCl_3$): 21.9 (Me), 160.4 (CH=N) ppm. ESI-HRMS: $m/z$ = 550.0857 (found), 550.0861 (calculated) for $[M+H_2O+H]^+$; 646.1554 (found), 646.1549 (calculated) for $[M+2MeCN+MeOH+H]^+$.

**3**, Yield: 0.17 g (66%); M.p.: 201–204 °C. IR (KBr)/cm$^{-1}$: $\nu_{asym}$ (CH=N): 1608.9. $^1$H NMR (500 MHz, $CDCl_3$): $\delta$ 2.27 (s, Me), 7.30–9.18 (m, aryl), 9.57 (s, CH=N). ESI-HRMS: $m/z$ = 532.0743 (found), 532.0756 (calculated) for $[M+H]^+$; 560.1510 (found), 560.1513 (calculated) for $[M(-Cl)+2MeOH]^+$. The $^{13}$C NMR of **3** could not be obtained due to its insufficient solubility.

*4.2.3. Synthesis of diorganotellurium dichlorides*

*4.2.3.1. Method-A: (**1a**, **1d**, **1e**, **2a–2c**, **3a** and **3b**).* A suspension of **1** (0.055 g, 0.100 mmol) and 4-MeO-$C_6H_4TeCl_3$ (0.034 g, 0.100 mmol) in chloroform (100 mL) were refluxed for 20 h with stirring under $N_2$. The hot reaction mixture was filtered to remove the precipitated $HgCl_2$. Concentration of the filtrate and addition of petroleum ether (40–60 °C) gave a solid which was recrystallized twice from $CHCl_3$ to obtain an orange-red solid of **1a**. Yield: 0.046 g (73%). M.p. 187 °C. IR (KBr)/cm$^{-1}$: $\nu_{asym}$ (CH=N): 1631.1. $^1$H NMR (400 MHz, DMSO-$d_6$): $\delta$ 2.31 (s, Me), 3.84 (s, OMe), 6.81–8.80 (m, aryl), 9.40 (s, CH=N) ppm). $^{13}$C NMR (500 MHz, DMSO-$d_6$): 21.0 (Me), 55.5 (OMe), 157.0 (CH=N) ppm. ESI-HRMS: $m/z$ = 572.0864 (found), 572.0869 (calculated) for $[M(-2Cl)+OH]^+$; 662.1313 (found), 662.0508 (calculated) for $[M+2H_2O+H]^+$. Anal. Calc. for $C_{31}H_{23}Cl_2NOTe$ (624.03): C, 59.67; H, 3.72; N, 2.24. Found: C, 59.43; H, 3.83; N, 2.35%.

Compounds **1d**, **1e**, **2a–2c**, **3a** and **3b** were prepared similarly.

**1d**: Yield: 0.037 g (63%). M.p. 171–173 °C. IR (KBr)/cm$^{-1}$: $\nu_{asym}$ (CH=N): 1615.4. $^1$H NMR (400 MHz, DMSO-$d_6$): $\delta$ 2.42 (s, Me), 7.19–8.42 (m, aryl), 9.38 (s, CH=N) ppm. $^{13}$C NMR (500 MHz, DMSO-$d_6$): 22.1 (Me), 153.2 (CH=N) ppm. ESI-HRMS: $m/z$ = 592.0926 (found), 592.0687 (calculated) for $[M(-Cl)+MeOH]^+$; 773.0131 (found), 773.1305 (calculated) for $[M+3H_2O+3MeCN+H]^+$. Anal. Calc. for $C_{30}H_{21}Cl_2NTe$ (594.00): C, 60.66; H, 3.56; N, 2.36. Found: C, 60.78; H, 3.38; N, 2.47%.

**1e**: Yield: 0.0.043 g (71%). M.p. 153–157 °C. IR (KBr)/cm$^{-1}$: $\nu_{asym}$ (CH=N): 1615.0. $^1$H NMR (400 MHz, DMSO-$d_6$): $\delta$ 2.48 (s, Me-SB), 2.33 (s, Me-tolyl-Te), 7.12–8.45 (m, aryl), 9.42 (s, CH=N) ppm. $^{13}$C NMR (500 MHz, DMSO-$d_6$): 22.1 (Me-SB), 28.7 (Me-tolyl-Te), 157 (CH=N) ppm. ESI-HRMS: $m/z$ = 610.2531 (found), 610.0348 (calculated) for $[M+H]^+$; 842.3364 (found), 842.1883 (calculated) for $[M+MeOH+4MeCN+2H_2O+H]^+$. Anal. Calc. for $C_{31}H_{23}Cl_2NTe$ (608.03): C, 61.24; H, 3.81; N, 2.30. Found: C, 61.33; H, 3.69; N, 2.17%.

**2a**. Yield: 0.043 g (71.6%). M.p. 179 °C. IR (KBr)/cm$^{-1}$: $\nu_{asym}$ (CH=N): 1625.3. $^1$H NMR (500 MHz, DMSO-$d_6$): $\delta$ 2.38 (s, Me), 3.90 (s, OMe), 7.13–9.02 (m, aryl), 10.15 (s, CH=N) ppm). $^{13}$C NMR (500 MHz, DMSO-$d_6$): 22.7 (Me), 55.6 (OMe), 158.6 (CH=N) ppm. ESI-HRMS: $m/z$ = 666.0837 (found), 666.0821 (calculated) for $[M+2MeOH+H]^+$; 630.1068 (found), 630.1055 (calculated) for $[M(-Cl)+2MeOH]^+$. 549.0857 (found), 548.0869 (calculated) for $[M(-2Cl+OH]^+$. Anal. Calc. for $C_{29}H_{23}Cl_2NOTe$ (600.01): C, 58.05; H, 3.86; N, 2.33. Found: C, 58.22; H, 3.71; N, 2.35%.

**2b**: Yield: 0.053 g (85%). M.p. 207–209 °C. IR (KBr)/cm$^{-1}$: $\nu_{asym}$ (CH=N): 1621.0. $^1$H NMR (500 MHz, DMSO-$d_6$): $\delta$ 2.48 (s, Me), 7.23–8.98 (m, aryl), 10.12 (s, CH=N) ppm. $^{13}$C NMR (500 MHz, DMSO-$d_6$): 23.4 (Me), 157.5 (CH=N) ppm. ESI-HRMS: $m/z$ = 622.0352 (found), 622.0348 (calculated) for $[M+H]^+$; 727.1489 (found), 727.1483 (calculated) for $[M(-Cl)+3MeCN+H_2O]^+$. Anal. Calc. for $C_{32}H_{23}Cl_2NTe$ (620.04): C, 61.99; H, 3.74; N, 2.26. Found: C, 62.34; H, 3.67; N, 2.32%.

**2c**: Yield: 0.039 g (63.7%). M.p. 169 °C. IR (KBr)/cm$^{-1}$: $\nu_{asym}$ (CH=N): 1602.8. $^1$H NMR (500 MHz, DMSO-$d_6$): $\delta$ 2.32 (s, Me-SB), 2.67 (s, Me-*o*-Mes), 2.12 (s, Me-*p*-Mes), 6.92–8.59 (m, aryl), 10.23 (s, CH=N) ppm. $^{13}$C NMR (500 MHz, DMSO-$d_6$): 23.5 (Me-SB), 28.8 (*p*-Me-mes), 30.3 (*o*-Me-mes), 162.7 (CH=N) ppm. ESI-HRMS: $m/z$ = 728.1454 (found), 728.1454 (calculated) for $[M+2MeCN+-MeOH+H]^+$. Anal. Calc. for $C_{31}H_{27}Cl_2NTe$ (612.06): C, 60.83; H, 4.45; N, 2.29. Found: C, 60.57; H, 4.35; N, 2.47%.

**3a**: Yield: 0.038 g (63%). M.p. 178 °C. IR (KBr)/cm$^{-1}$: $\nu_{asym}$ (CH=N): 1607.1. $^1$H NMR (500 MHz, DMSO-$d_6$): $\delta$ 2.49 (s, Me), 3.82 (s, OMe), 7.20–8.73 (m, aryl), 9.69 (s, CH=N) ppm). ESI-HRMS: $m/z$ = 757.1467 (found), 757.1455 (calculated) for $[M+MeCN+3-MeOH+H_2O+H]^+$; 620.0798 (found), 620.0847 (calculated) for $[M(-Cl)+3H_2O]^+$. Anal. Calc. for $C_{29}H_{23}Cl_2NOTe$ (600.01): C, 58.05;

H, 3.86; N, 2.33. Found: C, 58.42; H, 3.98; N, 2.23%. Insufficient solubility of **3a** precluded its $^{13}C$ NMR.

**3b**: Yield: 0.042 g (66%). M.p. 191–192 °C. IR (KBr)/cm$^{-1}$: $\nu_{asym}$ (CH=N): 1617.2. $^{1}H$ NMR (500 MHz, DMSO-$d_6$): $\delta$ 2.64 (s, Me), 7.24–9.46 (m, aryl), 10.38 (s, CH=N) ppm. $^{13}C$ NMR (500 MHz, DMSO-$d_6$): 21.2 (Me), 159.7 (CH=N) ppm. ESI-HRMS: $m/z$ = 636.1432 (found), 636.1394 (calculated) for [M(−2Cl)+MeOH+2H$_2$O+OH]$^+$. Anal. Calc. for $C_{32}H_{23}Cl_2NTe$ (620.04): C, 61.99; H, 3.74; N, 2.26. Found: C, 62.79; H, 3.75; N, 2.43%.

*4.2.3.2. Method-B: (**1b**, 1c and **3c**).* A suspension of **1** (0.055 g, 0.100 mmol) and 1-$C_{10}H_7TeCl_3$ (0.036 g, 0.100 mmol) in dry dioxane (50 mL) was heated under reflux until a clear solution was obtained. After cooling and evaporation to ~10 mL, diethyl ether (5 mL) was added. The solution was decanted off from a sticky mass. The latter was solvent extracted with hexane–$CHCl_3$ *via* a G-4 soxlet frit. Concentration of the extract, addition of petroleum ether (~5 mL) and cooling to 0 °C afforded an orange solid which was dissolved in chloroform (50 mL) and passed through a 4″ silica column. It was concentrated to half its volume and cooled below 0 °C for about two days affording pure **1b**.

Similar procedure was also applicable to **1c** and **3c**.

**1b**: Yield: 0.036 g (57%). M.p. 207–209 °C. IR (KBr)/cm$^{-1}$: $\nu_{asym}$ (CH=N): 1635.7. $^{1}H$ NMR (400 MHz, DMSO-$d_6$): $\delta$ 2.30 (s, Me), 7.19–8.22 (m, aryl), 9.40 (s, CH=N) ppm. $^{13}C$ NMR (500 MHz, DMSO-$d_6$): 22.5 (Me), 156.3 (CH=N) ppm. ESI-HRMS: $m/z$ = 687.0622 (found), 687.0614 (calculated) for [M+MeCN+H]$^+$. Anal. Calc. for $C_{34}H_{23}Cl_2NTe$ (644.06): C, 63.40; H, 3.60; N, 2.17. Found: C, 63.54; H, 3.78; N, 2.33%.

**1c**: Yield: 0.0.039 g (61%). M.p. 181–183 °C. IR (KBr)/cm$^{-1}$: $\nu_{asym}$ (CH=N): 1614.9. $^{1}H$ NMR (400 MHz, DMSO-$d_6$): $\delta$ 2.49 (s, Me-SB), 2.83 (s, Me-*o*-Mes), 2.25 (s, Me-*p*-Mes), 6.73–8.42 (m, aryl), 9.41 (s, CH=N) ppm. $^{13}C$ NMR (500 MHz, DMSO-$d_6$): 22.6 (Me-SB), 29.3 (*p*-Me-mes), 31.9 (*o*-Me-mes), 160.1 (CH=N) ppm. ESI-HRMS: $m/z$ = 765.1526 (found), 765.1506 (calculated) for [M+MeOH+-MeCN+3H$_2$O+H]$^+$; 804.9548 (found), 804.2809 (calculated) for [M(−2Cl)+mesityl+2MeCN+2H$_2$O]$^+$; 945.0184 (found), 945.2938 (calculated) for [M(−2Cl)+SB+MeCN+H$_2$O]$^+$. Anal. Calc. for $C_{33}H_{27}Cl_2NTe$ (636.08): C, 62.31; H, 4.28; N, 2.20. Found: C, 62.51; H, 4.22; N, 2.43%.

**3c**: Yield: 0.041 g (67%). M.p. 187 °C. IR (KBr)/cm$^{-1}$: $\nu_{asym}$ (CH=N): 1627.6. $^{1}H$ NMR (500 MHz, DMSO-$d_6$): $\delta$ 2.29 (s, Me-SB), 2.57 (s, Me-*o*-Mes), 2.21 (s, Me-*p*-Mes), 7.11–9.02 (m, aryl), 10.43 (s, CH=N) ppm. $^{13}C$ NMR (500 MHz, DMSO-$d_6$): 22.8 (Me-SB), 27.5 (*p*-Me-mes), 29.1 (*o*-Me-mes), 163.0 (CH=N) ppm. ESI-HRMS: $m/z$ = 650.0877 (found), 650.0872 (calculated) for [M+2H$_2$O+H]$^+$; 674.1643 (found), 674.1681 (calculated) for [M(−Cl)+3MeOH]$^+$. Anal. Calc. for $C_{31}H_{27}Cl_2NTe$ (612.06): C, 60.83; H, 4.45; N, 2.29. Found: C, 60.59; H, 4.47; N, 2.32%.

Note: The yields were lower when these reactions were carried out in chloroform instead of dioxane.

*4.2.4. X-ray crystallography*

All measurements for **1**, **1a**, **2a**, **2b** and **3b** were made on CCD Bruker SMART APEX diffractometer. Crystallographic data and refinement parameters are summarized in Table 1. Data were collected using a graphite-monochromated Mo Kα radiation ($\lambda_\alpha$ = 0.71073 Å). The program SMART [24] was used for collecting frames of data, indexing reflection, and determining lattice parameters, SAINT [24] for integration of the intensity of reflections and scaling, SADABS [25] for absorption correction and SHELXTL [26,27] for space group and structure determination. Full-matrix least-squares refinements on $F^2$, using all data, were carried out with anisotropic displacement parameters applied to all non-hydrogen atoms. Hydrogen atoms were included in geometrically calculated positions using a riding model and were refined isotropically. The figures were created using *Diamond* 3.1*d* software [28].

## Acknowledgments

V.C. is a Lalit Kapoor Professor of Chemistry. V.C. is thankful to the Department of Science and Technology for a J.C. Bose fellowship. A.K. thanks the Department of Science and Technology for Fast Track Young Scientists Fellowship. This work is also supported by the *Bioinorganic Chemistry Initiative*, DST, India.

## Appendix A. Supplementary material

CCDC 741238, 741239, 741240, 741214 and 741242 contain the supplementary crystallographic data for **1**, **1a**, **2a**, **2b** and **3b**. These data can be obtained free of charge from The Cambridge Crystallographic Data Centre via www.ccdc.cam.ac.uk/data_request/cif. Supplementary data associated with this article can be found, in the online version, at doi:10.1016/j.jorganchem.2009.09.030.

## References

[1] P. Knochel (Ed.), Handbook of Functionalized Organometallics, 1st ed., Wiley-VCH, Weinheim, 2005.
[2] V. Chandrasekhar, M.D. Pandey, P. Bag, S. Pandey, Tetrahedron 65 (2009) 4540–4546.
[3] V. Chandrasekhar, P. Thilagar, J.F. Bickley, A. Steiner, J. Am. Chem. Soc. 127 (2005) 11556–11557.
[4] G.L. Zheng, J.-F. Ma, Z.M. Su, L.K. Yan, J. Yang, Y.-Y. Li, J.F. Liu, Angew. Chem., Int. Ed. 43 (2004) 2409–2411.
[5] V. Chandrasekhar, S. Nagendran, S. Bansal, M.A. Kozee, D.R. Powell, Angew. Chem., Int. Ed. 39 (2000) 1833–1835.
[6] G.-L. Zheng, J.-F. Ma, J. Yang, Y.-Y. Li, X.-R. Hao, Chem. Eur. J. 10 (2004) 3761–3768.
[7] V. Chandrasekhar, K. Gopal, S. Nagendran, P. Singh, A. Steiner, S. Zacchini, J.F. Bickley, Chem. Eur. J. 11 (2005) 5437–5448.
[8] (a) J. Beckmann, P. Finke, M. Hesse, B. Wettig, Angew. Chem., Int. Ed. 47 (2008) 9982–9984;
(b) H. Rheinboldt, G. Vicentini, Chem. Ber. 89 (1956) 624–631;
(c) A.K.S. Chauhan, Anamika, A. Kumar, R.C. Srivastava, R.J. Butcher, A. Duthie, J. Organomet. Chem. 691 (2006) 5887–5894;
(d) N. Al-Salim, A.A. West, W.R. McWhinnie, T.A. Hamor, J. Chem. Soc., Dalton Trans. (1988) 2363–2371.
[9] (a) W.-Y. Wong, G.-L. Lu, L. Liu, J.-X. Shi, Z. Lin, Eur. J. Inorg. Chem. (2004) 2066–2077;
(b) L. Pauling, The Nature of the Chemical Bond, 3rd ed., Cornell University Press, New York, 1960. pp. 257–264.
[10] A.J. Canty, J.B. Deacon, Inorg. Chim. Acta 45 (1980) L225–L227.
[11] A.J. Canty, B.M. Gatehouse, J. Chem. Soc., Dalton Trans. (1976) 2018–2020.
[12] J.E. Huheey, E.A. Keiter, R.L. Keiter, Inorganic Chemistry: Principles of Structure and Reactivity, 4th ed., Harper Collins college Publishers, New York, 1993.
[13] Y. Wu, K. Ding, Y. Wang, Y. Zhu, L. Yang, J. Organomet. Chem. 468 (1994) 13–19.
[14] A.K.S. Chauhan, Anamika, Arun Kumar, R.C. Srivastava, R.J. Butcher, J. Beckmann, A. Duthie, J. Organomet. Chem. 690 (2005) 1350–1355.
[15] (a) K. Behera, M.D. Pandey, M. Porel, S. Pandey, J. Chem. Phys. 127 (2007) 184501–1845010;
(b) J.B. Birks, Photophysics of Aromatic Molecules, Wiley-Interscience, New York, NY, 1970.
[16] S.K. Kim, S.H. Lee, J.Y. Lee, R.A. Bartsch, J.S. Kim, J. Am. Chem. Soc. 126 (2004) 16499–16506.
[17] Y. Shiraishi, K. Ishizumi, G. Nishimura, T. Hirai, J. Phys. Chem. B 111 (2007) 8812–8822.
[18] A.I. Vogel, Vogel's Textbook of Practical Organic Chemistry, 5th ed., Longman, London, 1989.
[19] N.W. Alcock, W.D. Harrison, J. Chem. Soc., Dalton Trans. (1984) 869–875.
[20] W.R. McWhinnie, P. Thavornyutikarn, J. Chem. Soc., Dalton Trans. (1972) 551–554.
[21] J. Zukerman-Schpector, I. Haiduc, Cryst. Eng. Commun. 4 (2002) 178–193.
[22] R.L.O.R. Cunha, A.T. Omori, P. Castelani, F.T. Toledo, J.V. Comasseto, J. Organomet. Chem. 689 (2004) 3631–3636.
[23] K.P. Munshi, J. Inst. Chem. (India) 76 (2004) 49–51.
[24] SMART & SAINT Software Reference Manuals, Version 6.45; Bruker Analytical X-ray Systems, Inc., Madison, WI, 2003.
[25] G.M. Sheldrick, SADABS A Software for Empirical Absorption Correction; Ver. 2.05, University of Göttingen, Göttingen, Germany, 2002.
[26] SHELXTL Reference Manual, Ver. 6.1; Bruker Analytical X-ray Systems, Inc., Madison, WI, 2000.
[27] G.M. Sheldrick, SHELXTL Ver. 6.12, Bruker AXS Inc., Madison, WI, 2001.
[28] K. Bradenburg, Diamond, Ver. 3.1d, Crystal Impact GbR, Bonn, Germany, 2006.